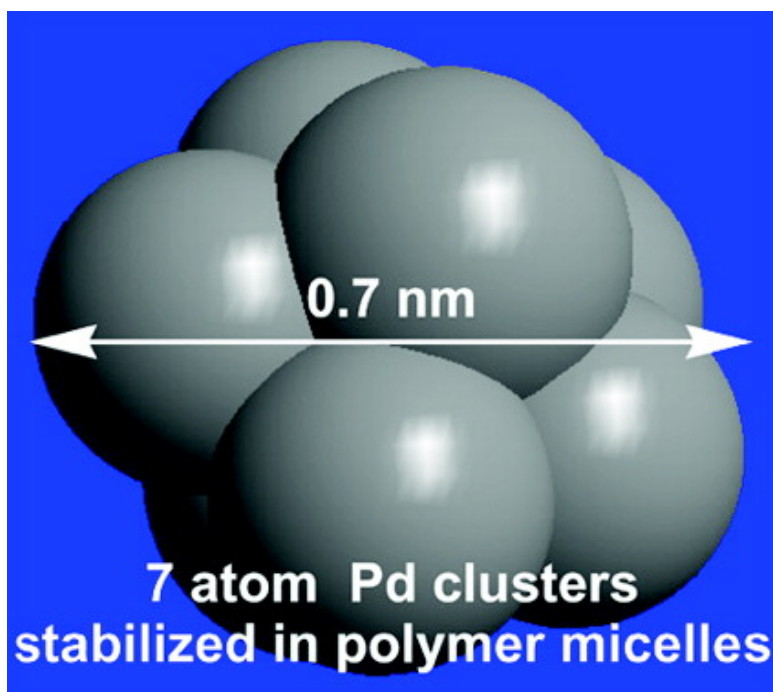


Formation of Nanoarchitectures Including Subnanometer Palladium Clusters and Their Use as Highly Active Catalysts

Kuniaki Okamoto, Ryo Akiyama, Hisao Yoshida, Tomoko Yoshida, and Sh Kobayashi

J. Am. Chem. Soc., **2005**, 127 (7), 2125-2135 • DOI: 10.1021/ja047095f • Publication Date (Web): 27 January 2005

Downloaded from <http://pubs.acs.org> on March 24, 2009



More About This Article

Additional resources and features associated with this article are available within the HTML version:

- Supporting Information
- Links to the 21 articles that cite this article, as of the time of this article download
- Access to high resolution figures
- Links to articles and content related to this article
- Copyright permission to reproduce figures and/or text from this article

[View the Full Text HTML](#)



ACS Publications
High quality. High impact.

Formation of Nanoarchitectures Including Subnanometer Palladium Clusters and Their Use as Highly Active Catalysts

Kuniaki Okamoto,[†] Ryo Akiyama,[†] Hisao Yoshida,[‡] Tomoko Yoshida,[§] and Shū Kobayashi^{*†}

Contribution from the Graduate School of Pharmaceutical Sciences, The University of Tokyo, Hongo, Bunkyo-ku, Tokyo 113-0033, Japan, Division of Environmental Research, EcoTopia Science Institute, Nagoya University, Nagoya 464-8603, Japan, and Division of Quantum Science and Energy Engineering, Department of Materials, Physics and Energy Engineering, Nagoya University, Nagoya 464-8603, Japan

Received May 18, 2004; E-mail: skobayas@mol.f.u-tokyo.ac.jp

Abstract: Subnanometer Pd clusters stabilized within micelles of random copolymers were formed by direct immobilization of Pd(0) via ligand exchange. The clusters were estimated to contain approximately seven Pd atoms on average (cluster diameter \approx 0.7 nm). Several Pd-containing micelle morphologies could be obtained by polymer cross-linking. These micelles containing Pd clusters were demonstrated to be efficient catalysts for hydrogenations and Heck reactions.

Introduction

Colloidal metal particles and metal clusters have attracted much interest because of their unique properties and potential applicability to microelectronics,¹ chemical sensing,² data storage,³ catalysts,⁴ etc. While smaller nanosized structure is desired in these fields, formation of nanoclusters necessarily requires stabilization to prevent aggregation, which would eradicate most of their desirable advantages compared with bulk materials of identical composition. Recently, a number of stabilizing methods have been developed for controlled formation of Pd nanoclusters.⁵ A standard strategy involves the use of weakly coordinated metals such as Pd(OAc)₂ and PdCl₂, which are complexes of a soft acid and a hard base, as starting materials. More stable complexes with softer bases of stabilizing agents (e.g., surfactants, functionalized polymers, dendrimers, or micelles of block copolymers) are then used to load the metals. Finally, the desired metal colloids are prepared by subsequent chemical reactions, typically reduction.⁶ The Pd nanoclusters thus prepared range in diameter from 1 to 40 or 50 nm. Among several preparation methods, the use of micelles of amphiphilic polymers to stabilize Pd clusters seems promising. Antonietti et al. reported the

formation of nanometer-sized Pd colloids in an amphiphilic block copolymer, polystyrene-*b*-poly-4-vinylpyridine.⁷ They used Pd(OAc)₂ as a precursor, which was first coordinated by a nitrogen atom of the polymer employed and then reduced to form the desired colloidal Pd. Several reducing agents were examined, which revealed that the size and the catalytic activity of the Pd colloids were influenced by the choice of reducing agents.⁷ It is also known that the stability of the polymer micelles and micellization behavior are influenced by several other factors, including concentration, temperature, and chemical structure of the polymer, and that various morphologies, such as spherical, rods, vesicles, and lamellae micelles, can be formed.⁸ In this article, we describe the formation of stable, subnanometer Pd clusters contained within micelles produced from random copolymers using a novel method. To the best of our knowledge, the Pd clusters formed in this work are the smallest reported to date (average cluster diameter \approx 0.7 nm). The clusters were stabilized in several micelle morphologies and exhibited efficient catalytic activity in hydrogenation and Heck reactions.

[†] The University of Tokyo.

[‡] EcoTopia Science Institute, Nagoya University.

[§] Department of Materials, Physics and Energy Engineering, Nagoya University.

- (1) (a) Schmid, G. *Chem. Rev.* **1992**, *92*, 1709–1727. (b) *Nanoparticles and Nanostructured Films*; Fendler, J. H., Ed.; Wiley-VCH: Weinheim, Germany, 1998. (c) Shipway, A. N.; Katz, E.; Willner, I. *Chem. Phys. Chem.* **2000**, *1*, 18–52. (d) Andres, R. P.; Bielefeld, J. D.; Henderson, J. I.; Janes, D. B.; Kolagunata, V. R.; Kubiak, C. P.; Mahoney, W. J.; Osifchin, R. G. *Science* **1996**, *273*, 1690–1693.
- (2) Emory, S. R.; Haskins, W. E.; Nie, S. *J. Am. Chem. Soc.* **1998**, *120*, 8009–8010.
- (3) Sun, T.; Seff, K. *Chem. Rev.* **1994**, *94*, 857–870.
- (4) (a) *Cluster and Colloids*; Schmid, G., Ed.; Wiley-VCH: Weinheim, Germany, 1994. (b) Lewis, L. N. *Chem. Rev.* **1993**, *93*, 2693–2730.
- (5) Beck, A.; Horváth, A.; Sárkány, A.; Guzzi, L. In *Nanotechnology in Catalysis*; Zhou, B., Hermans, S., Somorjai, G. A., Eds.; Kluwer Academic: New York, 2004; Vol. 1, Chapter 5.

- (6) (a) Förster, S.; Antonietti, M. *Adv. Mater.* **1998**, *10*, 195–217. (b) Lu, P.; Teranishi, T.; Asakura, K.; Miyake, M.; Toshima, N. *J. Phys. Chem. B* **1999**, *103*, 9673–9682. (c) Dutta, A. K.; Ho, T.; Zhang, L.; Stroeve, P. *Chem. Mater.* **2000**, *12*, 1042–1048. (d) Ding, J. H.; Gin, D. L. *Chem. Mater.* **2000**, *12*, 22–24. (e) Rheingans, O.; Hugenberg, N.; Harris, J. R.; Fischer, K.; Maskos, M. *Macromolecules* **2000**, *33*, 4780–4790. (f) Corbierre, M. K.; Cameron, N. S.; Sutton, M.; Mochrie, S. G. J.; Lurio, L. B.; Rühm, A.; Lennox, R. B. *J. Am. Chem. Soc.* **2001**, *123*, 10411–10412. (g) Pavel, F. M.; Mackay, R. A. *Langmuir* **2000**, *16*, 8568–8574. (h) Sohn, B. H.; Seo, B. H. *Chem. Mater.* **2001**, *13*, 1752–1757. (i) Hatano, T.; Takeuchi, M.; Ikeda, A.; Shinkai, S. *Org. Lett.* **2003**, *5*, 1395–1398.
- (7) Klingelhöfer, S.; Heitz, W.; Greiner, A.; Oestreich, S.; Förster, S.; Antonietti, M. *J. Am. Chem. Soc.* **1997**, *119*, 10116–10120.
- (8) (a) Zhang, L.; Eisenberg, A. *Science* **1995**, *268*, 1728–1731. (b) Henselwood, F.; Liu, G. *Macromolecules* **1997**, *30*, 488–493. (c) Harada, A.; Kataoka, K. *Science* **1999**, *283*, 65–67. (d) Jenekhe, S. A.; Chen, X. L. *Science* **1999**, *283*, 372–375. (e) Won, Y. Y.; Davis, H. T.; Bates, F. S. *Science* **1999**, *283*, 960–963. (f) Discher, B. M.; Won, Y. Y.; Ege, D. S.; Lee, J. C.-M.; Bates, F. S.; Discher, D. E.; Hammer, D. A. *Science* **1999**, *284*, 1143–1146. (g) Svensson, M.; Alexandridis, P.; Linse, P. *Macromolecules* **1999**, *32*, 637–645.

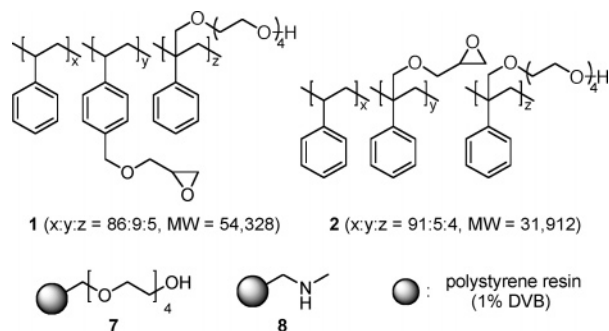


Figure 1. Compounds 1, 2, 7, and 8.

Results and Discussion

Recently, we have developed a new method for preparing immobilized catalysts using copolymer **1**, called the polymer incarcerated (PI) method (Figure 1). This method is based on microencapsulation⁹ and cross-linking. Tetrakis(triphenylphosphine)palladium(0) ($\text{Pd}(\text{PPh}_3)_4$) was immobilized using this method to form phosphine-free polymer incarcerated Pd(0) (PI Pd, **3a**).¹⁰ Electron probe microanalysis (EPMA) showed that Pd was dispersed throughout the polymer construct (Pd existed not only inside the structure but also close to the surface of the structure). Further, in this structure Pd(0) was assumed to be immobilized based on electronic interaction between π -electrons of the benzene rings of the polystyrene-based polymers and vacant orbitals of the palladium atoms.

While the PI Pd showed high catalytic activity in hydrogenation, allylation, and Suzuki–Miyaura coupling reactions, the structure of the Pd clusters was not well regulated. Our idea was that, if stable polymer micelles could be formed, smaller-sized, well-organized Pd(0) clusters could be generated.

Although copolymer **1** has an amphiphilic nature, it is hard to form clear micelles because hydrophilic epoxy branches are attached to the hydrophobic benzene rings. Therefore, we designed a new copolymer (**2**), which was expected to form clearer and more stable micelles by phase separation between the benzene rings and the epoxy or tetraethyleneglycol (TEG) moieties across the polymer backbone. Copolymer **2** was also expected to be able to adopt several micelle morphologies upon cross-linking between the epoxy and the alcohol moieties of the polymer side chains.

Copolymer **2** was synthesized by radical copolymerization of the corresponding vinyl monomers using 2,2'-azobis(isobutyronitrile) (AIBN) as an initiator. Polymerization was monitored by gas chromatography and ¹H NMR spectroscopy (Figures 2 and 3). It was found that the monomers were consumed at an almost constant rate from the initial stages to the end of the reaction and that the ratio of monomer units in the isolated polymer was also almost constant regardless of the total consumption (styrene/epoxy/TEG = 91/5/4). These results show that the polymerization proceeded in a random fashion.

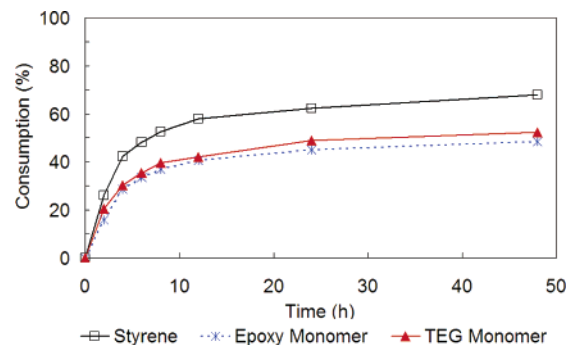


Figure 2. Plot of consumption versus time for each monomer during the polymerization. The consumptions were determined by GC analysis with reference to an internal standard (IS = methylcyclohexane).

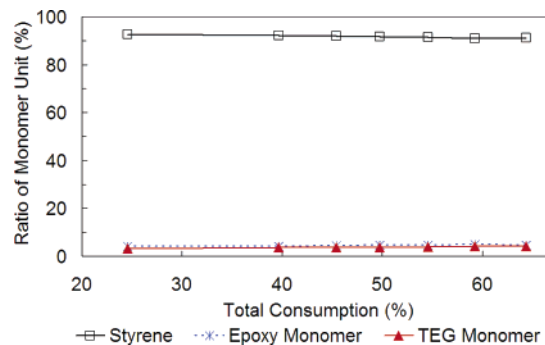


Figure 3. Plot of a ratio of monomer unit versus total consumption during the polymerization. The ratio of the monomer units was determined by ¹H NMR spectroscopy after isolation.

Copolymer **2** (500 mg) thus prepared and $\text{Pd}(\text{PPh}_3)_4$ (500 mg, 0.43 mmol) were then dissolved in dichloromethane (DCM, 10 mL), and *t*-amyl alcohol (*t*-AmOH) (50 mL) was slowly added to this solution. After being stirred for 8 h at room temperature, the mixture was observed by transmission electron microscopic (TEM) analysis. Very clear spherical micelles were formed, and the diameters of the micelles were 200–500 nm (Figure 4a). On the other hand, micelles prepared from copolymer **1** and $\text{Pd}(\text{PPh}_3)_4$ using the identical procedure are not spherical (Figure 4b). The different behavior of these polymers is thought to be due to the structural differences along the polymer backbone as mentioned previously.

The micelle solution prepared from copolymer **2** and $\text{Pd}(\text{PPh}_3)_4$ was heated at 120 °C for 5 h in a sealed tube to cross-link the polymer side chains and then poured into MeOH. The precipitate was collected by filtration and dried to afford Pd-containing solid (**4**). It is noted that 4 equiv of triphenylphosphineoxide were recovered from the filtrate. The TEM image of the resulting solid after dispersing in THF showed spherical micelles again (Figure 4c). It is presumed that the spherical nature of the micelles would be stabilized by intramicelle interactions. Judging from the magnified TEM image (Figure 4c, inset), we assumed that small Pd clusters were dispersed throughout the spherical micelles without the formation of large Pd clusters (TEM detection limit \approx 1 nm). The formation of extremely small Pd clusters was thought to be due to the stabilization of Pd clusters in the polymer micelles and the direct immobilization of Pd(0) by ligand exchange from triphenylphosphine to the benzene rings of the polymer. By comparison, when the cross-linking of Pd-containing polymer micelles was performed by microwave (MW) irradiation, 1–5-nm-sized clusters were observed and sphere shapes of the

- (9) (a) Kobayashi, S.; Akiyama, R. *Chem. Commun.* **2003**, 449–460. (b) Kobayashi, S.; Nagayama, S. *J. Am. Chem. Soc.* **1998**, *120*, 2985–2986. (c) Nagayama, S.; Endo, M.; Kobayashi, S. *J. Org. Chem.* **1998**, *63*, 6094–6095. (d) Kobayashi, S.; Endo, M.; Nagayama, S. *J. Am. Chem. Soc.* **1999**, *121*, 11229–11230. (e) Kobayashi, S.; Ishida, T.; Akiyama, R. *Org. Lett.* **2001**, *3*, 2649–2652. (f) Akiyama, R.; Kobayashi, S. *Angew. Chem., Int. Ed.* **2001**, *40*, 3469–3471. (g) Akiyama, R.; Kobayashi, S. *Angew. Chem., Int. Ed.* **2002**, *41*, 2602–2604. (h) Ishida, T.; Akiyama, R.; Kobayashi, S. *Adv. Synth. Catal.* **2003**, *345*, 576–579.
- (10) (a) Akiyama, R.; Kobayashi, S. *J. Am. Chem. Soc.* **2003**, *125*, 3412–3413. (b) Okamoto, K.; Akiyama, R.; Kobayashi, S. *J. Org. Chem.* **2004**, *69*, 2871–2873. (c) Okamoto, K.; Akiyama, R.; Kobayashi, S. *Org. Lett.* **2004**, *6*, 1987–1990.

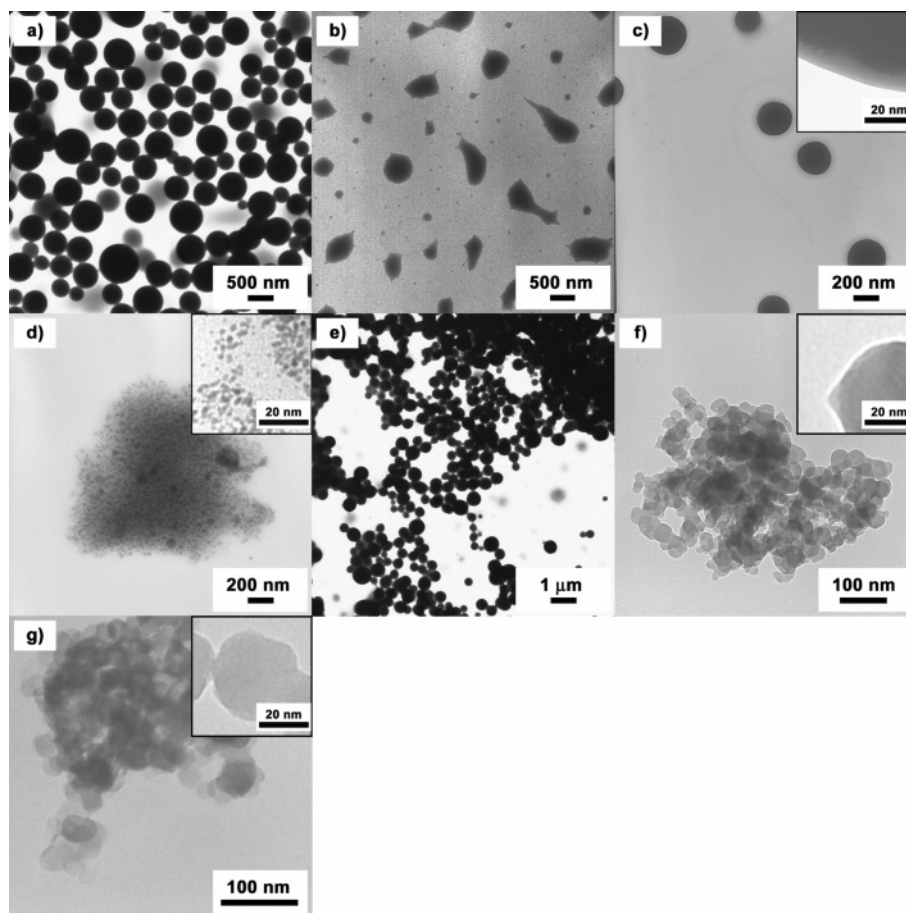


Figure 4. TEM images of Pd-polymer micelles. (a) Polymer (2)-Pd micelles in DCM/*t*-AmOH = 1/5. (b) Polymer (1)-Pd mixture in DCM/*t*-AmOH = 1/5. (c) Polymer (2)-Pd micelles cross-linked by conventional heating (4). (d) Polymer (2)-Pd mixture cross-linked by MW heating (5). (e) Polymer (2)-Pd micelles in DCM/MeOH = 1/1. (f) The networked polymer (2)-Pd micelles prepared in DCM/MeOH = 1/3 and cross-linked (6b). (g) 6b recovered after use in a Heck reaction.

micelles were disrupted (5, Figure 4d). It is already known that the stability of micelles and microemulsions is sensitive to several factors, such as temperature, pH, and addition of salts,⁸ and that emulsions can be destabilized by irradiation with MWs.¹¹ In our case, the polymer micelles were possibly destabilized by MW irradiation, and the interaction between the polymer and Pd was disrupted. Consequently, aggregation of the Pd clusters could occur.

We then examined morphological changes in the Pd-polymer micelles. In a MeOH/DCM solvent system, MeOH (10 mL) was slowly added to a DCM (10 mL) solution of the copolymer 2 (500 mg) and Pd(PPh₃)₄ (500 mg). Since MeOH is a poorer solvent for copolymer 2 than *t*-AmOH, aggregation of the micelles was observed (Figure 4e). Further addition of MeOH promoted the aggregation, and finally, Pd-polymer micelles were completely precipitated when the total amount of MeOH reached 30 mL (DCM/MeOH = 1/3). The precipitate was collected by filtration and dried in vacuo, and then the solid obtained was heated at 120 °C for 2 h without solvent. The resulting solid was washed with THF, *N*-methyl-2-pyrrolidinone (NMP), and DCM, successively, and insoluble Pd-containing solid (6b) was obtained (Figure 4f). The loading level of the Pd in this solid was determined to be 0.62 mmol/g.^{12,13} The structure of this

solid was observed by scanning electron microscopy (SEM) analysis after being freeze-dried from benzene, and the structure was found to be a porous three-dimensional (3-D) network (Figure 5a). The amount of the generated and remaining surface hydroxy groups of the networked solid (6b) was 117.8 μmol/g as determined by the photometrical quantitative analysis (see Experimental Section). On the other hand, although a similar 3-D network structure was also formed in the cross-linked solid (6a) prepared by a reverse-phase solvent system (hexane/THF = 3/1) in the micellization step, the amount of surface hydroxy groups of 6a was only 1.1 μmol/g. These results clearly indicate that the micelle integrity was maintained during the aggregation and cross-linking and that the network structure was formed by the constituents of the sphere and the rodlike micelles (diameter of sphere and rod = 20–50 nm). It is noteworthy that 3-D network structures were not formed in the cross-linked aggregates obtained by the same procedure without Pd (Figure 5b). This result supports that the morphology of the micelles was stabilized by interactions between Pd and the polymer.

X-ray Absorption Fine Structure (XAFS). Since the TEM image of 6b (Figure 4f, inset) did not reveal recognizable Pd cluster (presumably too small, TEM detection limit ≈ 1 nm), we chose to examine the structure by X-ray absorption near-edge structure (XANES) and extended X-ray absorption fine

(11) (a) Albinson, K. B.; Chalmers, W.; Aguayo, M. G.; McCaffrey, D. S., Jr. *Hydrocarbon Eng.* **2001**, *6*, 44–45. (b) Albinson, K. R. *World Refin.* **2001**, *11*, 41–43. (c) Maue, R.; Moll, F. *Acta Pharm. Technol.* **1987**, *33*, 225–230. (d) Petrowski, G. E. *J. Am. Oil Chem. Soc.* **1974**, *51*, 110–111.

(12) Determined by XRF analysis.

(13) Phosphorus content was 0.15% by elemental analysis.

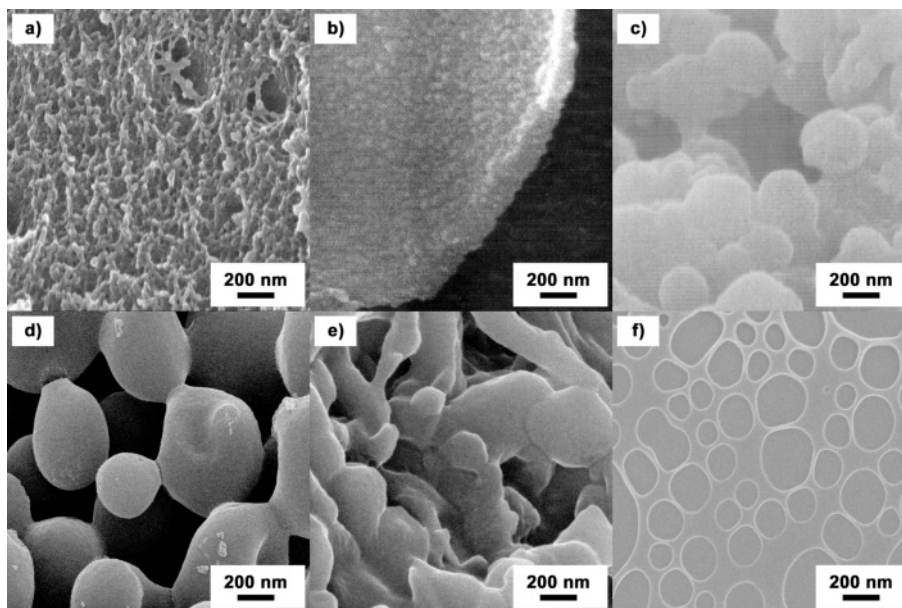


Figure 5. SEM images of solidified Pd-polymer micelles and polymer micelles. (a) The networked Pd-polymer micelles (**6b**). (b) Solidified polymer micelles without metal. (c) Pd-polymer micelles on the glass (**9**). (d) Pd-polymer micelles on hydroxylated resin (**10**). (e) Pd-polymer micelles on aminated resin (**11**). (f) Polymer micelles on the glass without metal.

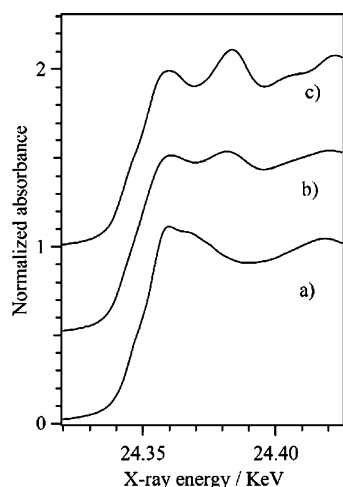


Figure 6. Pd K-edge XANES spectra of (a) PdO, (b) **6b**, and (c) Pd foil. structure (EXAFS). Figure 6 shows the Pd K-edge XANES spectra of PdO, Pd catalyst (**6b**), and Pd metal. Each spectrum was normalized by the height of the edge jump after removal of the contribution from absorption other than the K-edge absorption by Pd atoms.¹⁴ The spectrum feature in the post-edge region is higher than 24.36 keV and also reflected the local structure around the target Pd atom, that is, the coordination symmetry and electronic state of the Pd atom, as shown in the reference spectra (Figure 6a,c). The XANES spectrum of **6b** (Figure 6b) shows a similar feature to that of metallic Pd, which is characterized by two prominent peaks around 24.355 and 24.385 keV. This shows that **6b** has similar coordination symmetry to the Pd metal of face-centered cubic (fcc) structure. The spectrum of **6b** is clearly different from that of PdO. Note that the characteristic feature of the fcc metal in the spectrum of **6b** seems a little weak, suggesting that the Pd metal species in the catalyst would have a Pd metal fcc structure of very short-

range order, suggesting that very small Pd metal particles were formed in the polymer support.

Figure 7 shows k^3 -weighted Pd K-edge EXAFS spectra of PdO, **6b**, and Pd metal. The pattern of the EXAFS of **6b** is very similar to that of the reference Pd metal rather than that of PdO. However, the amplitude of the EXAFS of **6b** is much weaker than that of the Pd metal. The strong EXAFS oscillation of the Pd metal appears due to the well-arranged local structure of the fcc structure where 12 Pd atoms are coordinated at the same distance from the central Pd atom. When the size of Pd metal particles is small, there is a large fraction of unsaturated low coordination atoms, which explains the low amplitude of the EXAFS oscillation. Therefore, the EXAFS spectrum of **6b** (Figure 6b) implies that the sample has very small Pd metal particles.

Fourier transform (FT) was performed on the Pd K-edge EXAFS spectra in the $3\text{--}13 \text{ \AA}^{-1}$ region to obtain the radial structure function (RSF) as shown in Figure 8. A peak observed at $2\text{--}4 \text{ \AA}$ shows the presence of first- or second-neighboring Pd atoms. It is noteworthy that the peaks due to the Pd atoms for **6b** (Figure 8b) and the reference Pd metal (Figure 8c) appeared at the same position. This confirms that the Pd of **6b** was in a metallic environment. However, the peak magnitude for **6b** was much lower than that for the reference Pd metal. This result demonstrates a decrease in the number of neighboring Pd atoms, supporting the presence of small Pd metal particles in **6b**, and the RSF peaks appearing around 1.6 \AA are due to the backscattering from adjacent carbon or oxygen atoms. In the RSF of PdO, the peak around 1.6 \AA is assignable to the Pd–O shell. In the RSF of **6b**, a very small peak can be observed in a similar position, which is probably due to carbon atoms of polymers coordinated with Pd atoms (Pd–C shell) or oxygen atoms on the surface of Pd metal particles (Pd–O shell) (vide infra).

To clarify the local structure around the Pd atoms of **6b**, we performed nonlinear curve-fitting analyses of the Fourier-filtered EXAFS of the first and the second shells, corresponding to

(14) Tanaka, T.; Yamashita, H.; Tsuchitani, R.; Funabiki, T.; Yoshida, S. *J. Chem. Soc., Faraday Trans. 1* **1988**, *84*, 2987–2999.

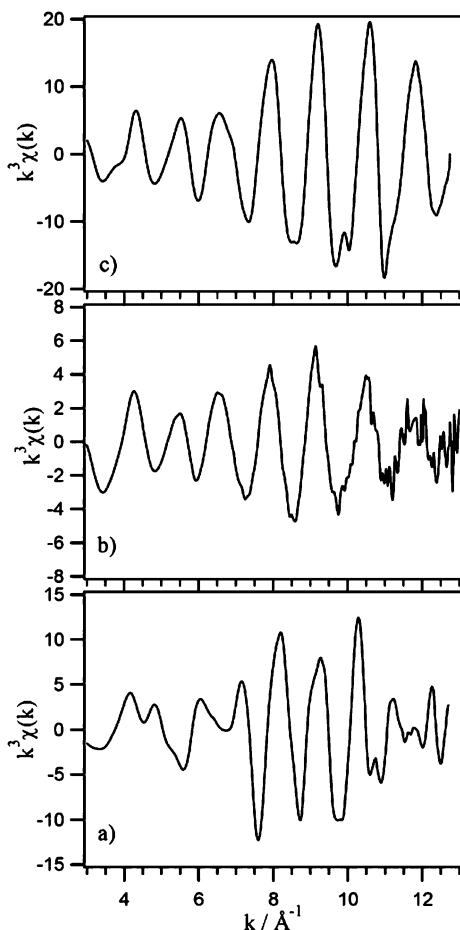


Figure 7. k^3 -Weighted Pd K-edge EXAFS of (a) PdO, (b) **6b**, and (c) Pd foil.

Pd–C (or Pd–O) and Pd–Pd shells, by a least-squares method. For Fourier-filtering, a set of the peaks in a RSF in Figure 8 was isolated with a Hanning window in the region of 1.1–2.9 Å and was inversely Fourier-transformed. The curve-fitting analysis was carried out in the region of 3–13 Å⁻¹, using the following eq 1:

$$k\chi(k) = \sum A_j(k) \times N_j/r_j^2 \times \exp(-2\Delta\sigma_j^2 k^2) \sin(2kr_j + \phi_j(k)) \quad (1)$$

where N_j is the coordination number of scattering atoms at distance r_j , and $\Delta\sigma_j^2$ is the difference between the Debye–Waller factors of a sample of interest and a reference sample. The amplitude $A(k)$ and phase shift $\phi(k)$ for Pd–O or Pd–Pd were extracted from the EXAFS spectrum of a PdO powder and a Pd metal foil, respectively. The curve-fitting results are given in Table 1, and the fit for **6b** is shown in Figure 9. From this analysis for **6b**, the interatomic distance of the Pd–Pd shell was estimated to be 2.76 Å, which was almost consistent with that of the reference Pd metal. The coordination number (CN) was calculated to be 4.4, which was much lower than that in the reference Pd metal, suggesting that the size of the Pd metal in **6b** is extremely small.

A sphere-like particle of the fcc structure was considered as a stable model cluster¹⁵ to estimate the cluster size of Pd metal

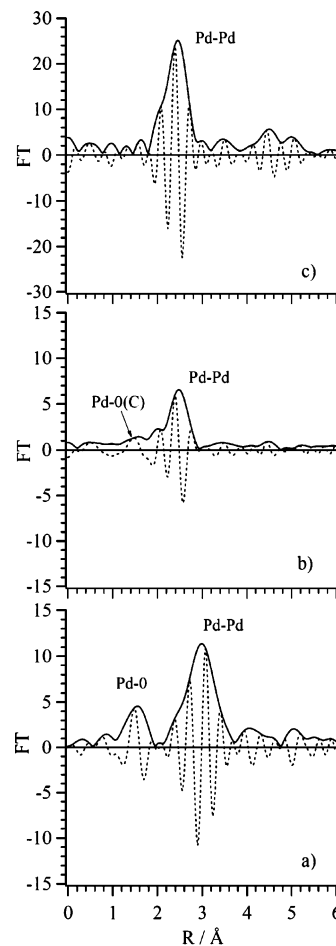


Figure 8. FT of k^3 -weighted Pd K-edge EXAFS of (a) PdO, (b) **6b**, and (c) Pd foil.

Table 1. Curve-Fitting Analyses of the Fourier-Filtered EXAFS^a

sample	shell	coordination number	interatomic distance (Å)	$\Delta\sigma^2$ ^b (Å ²)	RF ^c (%)
PdO	Pd–O	4.0	2.01	0	9.7
	Pd–Pd	4.0	3.05	–0.00010	
	Pd–Pd	8.0	3.43	–0.00024	
6b	Pd–O (C)	1.0	1.96	–0.00172	8.8
	Pd–O (C)	1.2	2.14	–0.00159	
	Pd–Pd	4.4	2.76	0.00192	
	Pd–Pd	12.0	2.75	0	

^a The region of 1.1–2.9 Å in RSF of the Pd catalyst sample (**6b**) was inversely Fourier transformed. The Pd–O and Pd–Pd shells were extracted from EXAFS of a PdO powder and a Pd metal foil, respectively. The errors in coordination number and interatomic distance are $\pm 20\%$ and ± 0.02 Å, respectively. ^b $\Delta\sigma^2$ is the difference between the Debye–Waller factors of the catalyst sample and the reference samples (PdO and Pd foil). ^c RF(%) = $\{[\sum_k(\chi_{\text{exp}}(k) - \chi_{\text{calcd}}(k))^2]/[\chi_{\text{exp}}(k)^2]^{1/2}\} \times 100$

from the coordination number. The Pd–Pd distance employed was 0.275 nm. For example, a cluster consisting of 13 atoms as cubotetrahedron has a diameter of 0.825 nm, which shows 5.53 as coordination number, while octahedron consisting of 19 atoms is 1.05 nm in size and CN should be 6.32. In this way, geometrical calculation was carried out on some stable clusters, and the results are plotted in Figure 10. The cluster whose coordination number was 4.4 would be larger than the four-atom tetrahedra and smaller than the 13-atom cubotetrahedron; the estimated number of Pd in **6b** was around seven and the diameter was around 0.7 nm on average, indicating the formation of subnanometer Pd metal clusters.^{16,17} The results

(15) (a) Westergren, J.; Nordholm, S.; Rosén, A. *Eur. Phys. J. D* **2003**, *22*, 81–97. (b) Watari, N.; Ohnishi, S. *Phys. Rev. B* **1998**, *58*, 1665–1677.

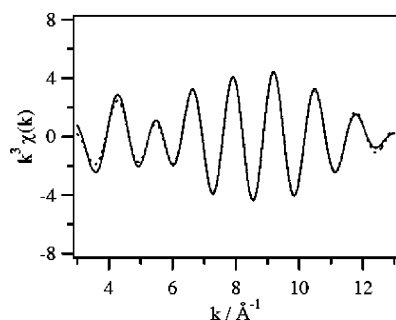


Figure 9. Fit of Fourier-filtered EXAFS of **6b**. The solid curve is obtained experimentally, and the dotted curve is the calculated fit.

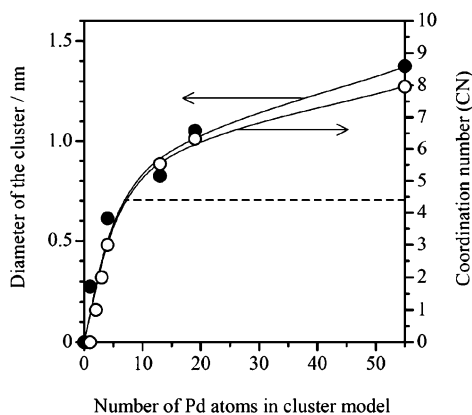
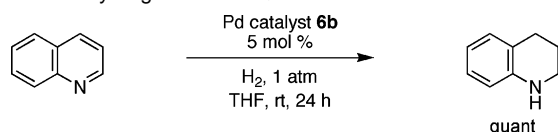


Figure 10. Geometrical calculation of the diameter of small sphere Pd cluster and the average coordination number in the cluster.

Scheme 1. Hydrogenation of Quinoline



from the curve-fitting analysis for the first shell (Table 1) indicated that the first neighboring atom would be a carbon of the polymer support in addition to possible surface oxygen of the Pd cluster since two kinds of atomic distance for the first shell were required to fit; their interatomic distances and coordination numbers are estimated as (1.96 Å, 1.0) and (2.14 Å, 1.2). Quite recently, the structure of the perylene-tetrapalladium sandwich complex has been revealed by X-ray crystal structure analyses, and they elucidated that the Pd–C distance of this complex was 2.142–2.467 Å.¹⁸ This distance is close to that of Pd–O (C) of **6b** shown in Table 1. These data suggest that the subnanometer Pd clusters would be attached to the polymer support.

Catalysis. It was found that the networked Pd micelles (**6b**) catalyzed the hydrogenation of quinoline to afford 1,2,3,4-tetrahydroquinoline quantitatively under hydrogen at atmospheric pressure and room temperature (Scheme 1). The kinetic profile of the reduction is shown in Figure 11. It is noted that no induction period was observed. These results and the previous XAFS data would suggest the presence of Pd(0) in **6b**.

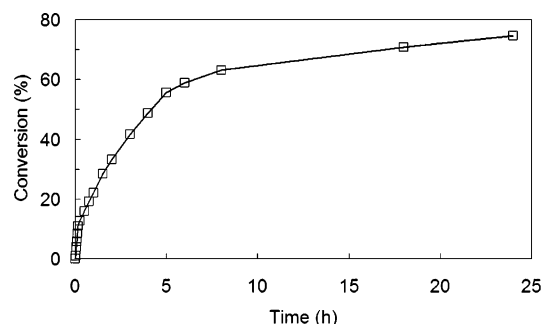


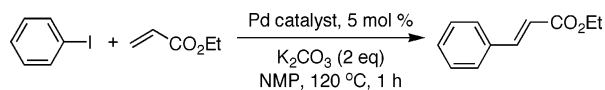
Figure 11. Plot of conversion versus time for the hydrogenation of quinoline. The conversions were determined by GC analysis with reference to an internal standard (IS = decane). Reaction conditions: Quinoline (1 mmol), **6b** (1 mol %), THF (10 mL), decane (50 μL), and H₂ (1 atm) at room temperature.

Next, we examined catalytic activities of the Pd micelles in the Heck reaction of iodobenzene with ethyl acrylate;¹⁹ the results are summarized in Table 2. When PI Pd (from copolymer **1**) prepared in either solvent system (hexane/THF (**3a**) and MeOH/DCM (**3b**)) was used, the same level of leaching of the Pd to the reaction mixture was observed. In both PI Pd **3a** and **3b**, Pd coordinated with the benzene rings of the polymers was thought to exist both inside and outside of the structure. On the other hand, while the networked Pd-polymer micelles **6b** did not show any leaching at all, the micelles **6a** showed significant leaching of Pd. These results indicate that Pd was located in the hydrophobic part of the micelles (inside for **6b** and outside for **6a**).

On the other hand, the micelles containing Pd could be fixed on several supports such as a glass surface, a hydroxylated resin (**7**), or an aminated resin (**8**), which would be also used as catalysts (see Figure 5c–e). The SEM images of the plain supports are shown in Figure 12). To a solution of the Pd-polymer micelles in the *t*-AmOH/DCM system, a glass, hydroxylated resin (**7**), or aminated resin (**8**) was added, and the mixtures were allowed to stand overnight to allow precipitation of the micelles onto the supports. The supports with the micelles were washed with MeOH and then dried and heated at 120 °C for 2 h. After being washed with THF, spherical micelles were observed on the glass (**9**, Figure 5c) and the hydroxylated resin (**10**, Figure 5d). It was assumed that the immobilization of the micelles onto the supports by binding the epoxides to silanols on the glass or the alcohols on the resin and cross-linking of the polymer side chains occurred by heating at 120 °C at the same time. In the case of the aminated resin, the micelle morphology partially changed to a rodlike structure (**11**, Figure 5e). Since the epoxides of polymer **2** would react with the amine moieties on the resin before cross-linking of the polymer side chains, the morphology might be partially changed. Subsequent heating at 120 °C led to the morphologies of the micelles being fixed by the cross-linking of the polymer side chains. Conversely, the aggregates of the micelles of polymer **2** without Pd on a glass did not form micelles, but rather a membrane was observed (Figure 5f). This result also

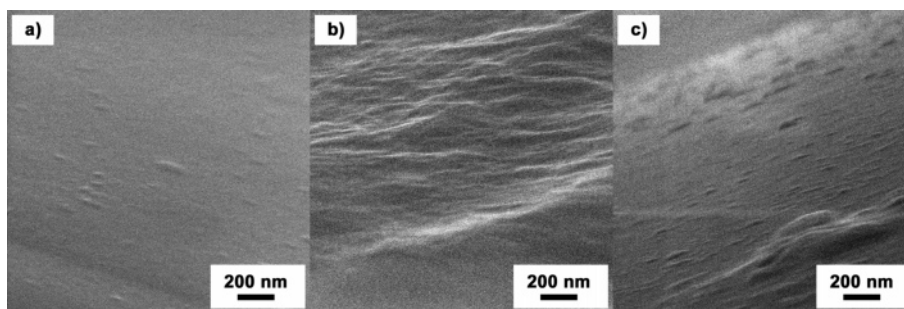
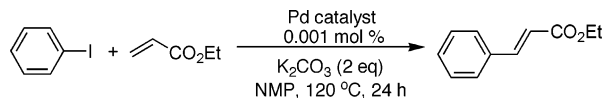
(16) Structure of Pd_n clusters ($n = \sim 2-7$) was proposed based on density functional theory. Bertani, V.; Cavallotti, C.; Masi, M.; Carrá, S. *J. Phys. Chem. A* **2000**, *104*, 11390–11397.
 (17) Small but rather unstable Pd clusters were produced on the surface of supports by vapor deposition. Henry, C. R. *Surf. Sci. Rep.* **1998**, *31*, 231–325.
 (18) Murahashi, T.; Uemura, T.; Kurosawa, H. *J. Am. Chem. Soc.* **2003**, *125*, 8436–8437.

(19) Review: (a) Reetz, M. T.; de Vries, J. G. *Chem. Commun.* **2004**, *14*, 1559–1563. (b) Beletskaya, I. P.; Cheprakov, A. V. *Chem. Rev.* **2000**, *100*, 3009–3066. (c) Heck, R. F. In *Comprehensive Organic Synthesis*; Trost, B. M., Fleming, I., Eds.; Pergamon Press: Oxford, 1991; Vol. 4. (d) De Meijere, A.; Braese, S. In *Transition Metal Catalyzed Reactions*; Davies, S. G., Murahashi, S.-I., Eds.; Blackwell Science: Oxford, 1999. (e) Link, J. T.; Overman, L. E. In *Metal-Catalyzed Cross-Coupling Reactions*; Diederich, F., Stang, P. J., Eds.; Wiley-VCH: New York, 1998.

Table 2. Heck Reaction Using Pd-Containing Micelles, the Effect of Polymer and Solvent System

entry	Pd catalyst ^a	solvent system ^b	observed structure ^c	diameter of micelles ^c (nm)	yield of cinnamate ^d	Pd leaching ^e (ppm)
1	3a	hexane/THF	networked	20–50	87	78.7
2	3b	MeOH/DCM	networked	20–50	80	71.8
3	6a	hexane/THF	networked	20–50	88	92.0
4	6b	MeOH/DCM	networked	20–50	93	nd

^a The loading of Pd was determined by XRF analysis after decomposition. **3a**: 0.81 mmol/g, **3b**: 0.67 mmol/g, **6a**: 0.65 mmol/g, **6b**: 0.62 mmol/g. ^b Solvents for micellization. The ratio of poor solvent to good solvent was 3 to 1. ^c Determined by TEM observation. ^d Isolated yield. ^e The concentration of leached Pd was measured by XRF analysis. nd: not detected (<5 ppm).

**Figure 12.** SEM images of plain supports (with no copolymer and Pd loading). (a) Glass, (b) hydroxylated resin (**7**), and (c) aminated resin (**8**).**Table 3.** Heck Reaction Using Various Pd-Containing Micelles

entry	Pd catalyst ^a	solvent system ^b	observed structure ^c (nm)	diameter micelles ^c (%)	yield of cinnamate ^d	TON ^e
1	3a	hexane/THF	networked	20–50	52	52 300
2	4	<i>t</i> -AmOH/DCM	sphere	200–500	81	81 400
3	5	<i>t</i> -AmOH/DCM	broken ^f	–	19	19 400
4	6b	MeOH/DCM	networked	20–50	83	82 500
5	10	<i>t</i> -AmOH/DCM	sphere	200–500	78	78 200
6	11	<i>t</i> -AmOH/DCM	sphere, rod ^g	100–500	65	64 500
7	5% Pd/C	–	–	–	31	30 800

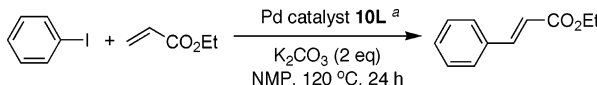
^a The loading of Pd was determined by XRF analysis after decomposition. **4**: 0.81 mmol/g, **5**: 1.73 mmol/g, **6b**: 0.62 mmol/g, **10**: 0.009 mmol/g, **11**: 0.037 mmol/g. ^b Solvents for micellization. The ratio of solvents was 5 to 1 for *t*-AmOH/DCM and 3 to 1 for MeOH/DCM and hexane/THF. ^c Determined by TEM observation. ^d Isolated yield. ^e TON: turnover number. ^f The micelles were disrupted, and 1 to 5 nm sized Pd clusters were observed. ^g Cross-linked sphere or rod micelles were observed.

suggests that the micelles were stabilized by interaction between Pd and the polymer.

Next, we compared catalytic activities of the various micelles in the Heck reaction. While PI Pd **3a** and the disrupted micelles **5** obtained by MW irradiation gave lower yields, all of the other cross-linked Pd micelles exhibited considerably high catalytic activities; the catalytic turnover numbers (TONs) were greater than 60 000 (Table 3, entries 2, 4, 5, and 6). Pd/C (5%) gave lower yield and TON. It is noteworthy that, despite the considerable difference in the shapes of the various micelles, the catalytic activities were almost the same. This indicates that the surface area of the catalyst construct hardly affects the catalytic activity. Remarkably high catalytic activity was observed using low loading micelle catalyst **10L**, which was prepared according to the same procedure as that of **10** except for the amount of the resin (a 5-fold increase of resin **7** was used as a support) and the TON was over 280 000 (Table 4, entry 3).²⁰ Moreover, catalyst **10L** could be reused without significant loss of activity at 0.001 mol % (Table 4, entry 2).

Although leaching of Pd to the reaction mixture was not detected by fluorescence X-ray (XRF) analysis in this system, the detection limit (5 ppm) was not sufficient to deny the possibility that a very small amount of leached Pd catalyzed the reaction. We then carefully checked the catalytic activity of the filtrate. After the coupling reaction of iodobenzene

- (20) TOF = 11 800. TON and TOF in other immobilized Pd including nanoparticles. (a) Yamada, Y. M. A.; Takeda, K.; Takahashi, H.; Ikegami, S. *Tetrahedron* **2004**, *60*, 4097–4105 (TON = 1 150 000, TOF = 12 000; iodobenzene and methyl acrylate). (b) Mandal, S.; Roy, D.; Chaudhari, R. V.; Sastry, M. *Chem. Mater.* **2004**, *16*, 3714–3724 (TOF = 4256; iodobenzene and styrene). (c) Hagiwara, H.; Sugawara, Y.; Isobe, K.; Hoshi, T.; Suzuki, T. *Org. Lett.* **2004**, *6*, 2325–2328 (TON = 68 400, TOF = 8 000; iodobenzene and cyclohexyl acrylate). (d) Mori, K.; Yamaguchi, K.; Hara, T.; Mizugaki, T.; Ebitani, K.; Kaneda, K. *J. Am. Chem. Soc.* **2002**, *124*, 11572–11573 (TON = 49 000; 4'-iodoacetophenone and butyl acrylate). (e) Köhler, K.; Heidenreich, R. G.; Krauter, J. G. E.; Pietsch, J. *Chem.–Eur. J.* **2002**, *8*, 622–631 (TON = 18 000, TOF = 9 000; bromobenzene and styrene). (f) Rahim, E. H.; Kamounah, F. S.; Frederiksen, J.; Christensen, J. B. *Nano. Lett.* **2001**, *1*, 499–501 (TON = 36 800, TOF = 3066; 1-bromo-2-iodo-benzene and acrylic acid). (g) Le Bars, J.; Specht, U.; Bradley, J. S.; Blackmond, D. G. *Langmuir* **1999**, *15*, 7621–7625 (TON = 100 000, TOF = 80 000; 4-Br-benzaldehyde and butyl acrylate). (h) Reference 7 (TON = 56 600; 4'-bromoacetophenone and styrene).

Table 4. Minimized Catalyst and Reuse


entry	Pd catalyst 10L (mol%)	yield of cinnamate ^b	TON ^c
1	0.001	93	93 400
2 ^d	0.001	90	90 000
3	0.0003	85	284 660

^a **10L** was prepared by the same procedure for **10** except for the amount of resin **7** (5-fold increase). The loading of palladium in **10L** was determined by XRF analysis after decomposition: 0.8 μmol/g. ^b Isolated yield. ^c TON: turnover number. ^d Recovered catalyst from entry 1 was used.

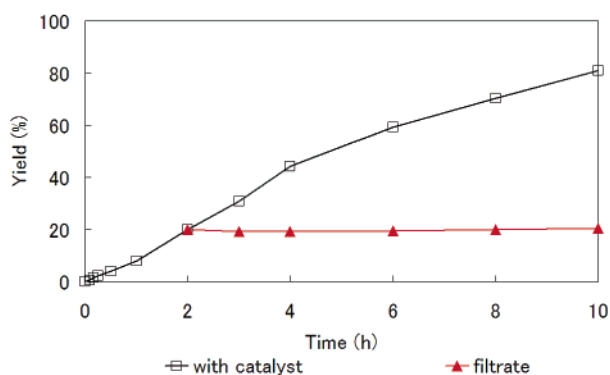
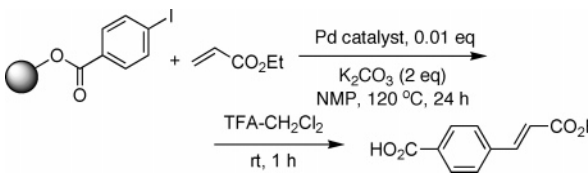


Figure 13. Plot of yield versus time for the Heck reaction. The yields were determined by GC analysis with reference to an internal standard (IS = dodecane). Reaction conditions: Iodobenzene (50 mmol), ethyl acrylate (75 mmol), **6b** (0.01 mol %), K₂CO₃ (100 mmol), NMP (50 mL), and dodecane (2.5 mL) at 120 °C. For the filtrate test, the catalyst was removed by hot filtration^a after 2 h (20% yield), and the experiment was continued with the filtrate in the presence of additional K₂CO₃ (2 equiv). ^aThe filtration was carried out while hot to avoid Pd deposition using a glass syringe coupled with a disk filter (0.45 μm PTFE membrane, 25 mm diameter; Whatman, Inc.).

(50 mmol) with ethyl acrylate (75 mmol) in the presence of 0.01 mol % of **10L** and potassium carbonate (100 mmol) in NMP (50 mL), the catalyst was removed by simple filtration. To the filtrate were added iodobenzene (50 mmol), ethyl acrylate (75 mmol), and potassium carbonate (100 mmol) again, and the mixture was further stirred for 24 h at 120 °C. No additional formation of the Heck product was observed, thus indicating no Pd leaching occurred. We also conducted a kinetic study and a hot leaching test.²¹ The profile of the reaction between iodobenzene and ethyl acrylate and the result of the leaching test are shown in Figure 13. The kinetic profile shows a short induction period, and it is noted that a similar kinetic profile was observed in the Heck reaction using Pd(OAc)₂.²² The reaction did not proceed at all after hot filtration (hot leaching test) of the catalyst. These results suggest that an active Pd species for the Heck reaction may be produced in the initial stages of the reaction and that the active species may exist not in a solution but inside the support.

Further evidence that no Pd leaching occurred was garnered from experiments based on the “three-phase tests”²³ consisting of anchoring one of the substrates onto a solid support in addition to using the solid catalyst. If an active species is really heterogeneous, transformation should be hardly observed for

- (21) Lipshutz, B. H.; Tasler, S.; Chrisman, W.; Spliethoff, B. Tesche, B. *J. Org. Chem.* **2003**, *68*, 1177–1189.
 (22) de Vries, A. H. M.; Mulders, J. M. C. A.; Mommers, J. H. M.; Henderickx, H. J. W.; de Vries, J. G. *Org. Lett.* **2003**, *5*, 3285–3288.

Table 5. Three-Phase Test


entry	Pd catalyst	yield of cinnamate ^b (%)
1	6b ^a	2
2	5% Pd/C	10
3	Pd(PPh ₃) ₄	48

^a The loading of palladium: 0.62 mmol/g. ^b Determined by ¹H NMR analysis.

the anchored substrate. We prepared Wang Resin-bounded aryl iodide,²⁴ which was then employed in Heck reactions with ethyl acrylate in the presence of **6b**, 5% Pd/C, or Pd(PPh₃)₄ (Table 5). While Pd(PPh₃)₄ gave the Heck adduct in 48% yield after cleavage from the support, the adducts were obtained in only 2 and 10% yields using **6b** and Pd/C, respectively. Although a very small amount of Pd might exist in the solution when **6b** was used in this “three-phase test” (which promoted the Heck reaction to afford the adduct in 2% yield), the result of the hot leaching test mentioned above indicates that no active species exist in the solution. These results suggest that most of the active Pd species were held inside the micelles and that catalytic turnover predominantly took place there too.

In Heck reactions using heterogeneous Pd(0) clusters such as Pd/C, Pd/Al₂O₃, Pd/SiO₂, etc., several research groups observed leaching of Pd²⁵ and suggested a soluble molecular Pd species was the true catalyst. According to the generally accepted mechanism for the Heck reaction, Pd(II) complexes with substrates that are conceivably soluble exist in a catalytic cycle. In our system, the fact that dissolved active Pd species did not seem to exist in the solution phase of the reaction mixture and that the surface area of the micelle catalyst minimally affected the catalytic activity suggest that most substrates would localize in hydrophobic environments created by the polymer micelles and that the coupling reactions and regeneration of Pd(0) would proceed inside the micelles. The TEM image of recovered **6b** after Heck reaction (Figure 4g), which indicates almost the same structure as that of fresh **6b** and existence of subnanometer Pd clusters, may support this mechanism, because regeneration and aggregation of Pd(0) in a solution without stabilizer would lead to formation of large Pd clusters. Thus, these Pd-polymer micelles could serve as a nanoreactor.

- (23) (a) Rebek, J.; Gavina, F. *J. Am. Chem. Soc.* **1974**, *96*, 7112–7114. (b) Rebek, J.; Broun, D.; Zimmerman, S. *J. Am. Chem. Soc.* **1975**, *97*, 454–455. (c) Collman, J. P.; Kosydar, K. M.; Bressan, M.; Lamanna, W.; Garrett, T. *J. Am. Chem. Soc.* **1984**, *106*, 2569–2579. (d) Davies, I. W.; Matty, L.; Hughes, D. L.; Reider, P. J. *J. Am. Chem. Soc.* **2001**, *123*, 10139–10140. (e) Widegren, J. A.; Finke, R. G. *J. Mol. Catal. A: Chem.* **2003**, *198*, 317–341. (f) Baleizão, C.; Corma, A.; Garcia, H.; Leyva, A. *J. Org. Chem.* **2004**, *69*, 439–446. (g) Yu, K.; Sommer, W.; Weck, M.; Jones, C. W. *J. Catal.* **2004**, *226*, 101–110. (h) See also ref 21.
 (24) (a) Yu, K.-L.; Deshpande, M. S.; Vyas, D. M. *Tetrahedron Lett.* **1994**, *35*, 8919–8922. (b) Hiroshige, M.; Hauske, J. R.; Zhou, P. *Tetrahedron Lett.* **1995**, *36*, 4567–4570. (c) Brase, S.; Kirchoff, J. H.; Kobberling, J. *Tetrahedron* **2003**, *59*, 885–939.
 (25) (a) Zhao, F.; Murakami, K.; Shirai, M.; Arai, M. *J. Catal.* **2000**, *194*, 479–483. (b) Köhler, K.; Wagner, M.; Djakovitch, L. *Catal. Today* **2001**, *66*, 101–110. (c) Heidenreich, R. G.; Krauter, J. G. E.; Pietsch, J.; Köhler, K. *J. Mol. Catal. A: Chem.* **2002**, *182–183*, 499–509. (d) Zhao, F.; Bhanage, B. M.; Shirai, M.; Arai, M. *Chem.-Eur. J.* **2000**, *6*, 843–848. (e) Choudary, B. M.; Madhi, S.; Chowdari, N. S.; Kantam, M. L.; Sreedhar, B. *J. Am. Chem. Soc.* **2002**, *124*, 14127–14136. (f) See also refs 20e and 21.

Experimental Section

General. ^1H and ^{13}C NMR spectra were recorded on a JEOL JNM-LA300, JNM-LA400 spectrometer in CDCl_3 unless otherwise noted. Tetramethylsilane was used as an internal standard ($\delta = 0$) for ^1H NMR, and the CDCl_3 solvent peak was used as the internal standard ($\delta = 77.0$) for ^{13}C NMR. 2-Phenylpropene, *N*-bromosuccinimide (NBS), bromobenzene, glycidol, styrene, tetraethyleneglycol, α -naphthylisocyanate, quinoline, iodobenzene, and 4-(dimethylamino)pyridine were purchased from Tokyo Chemical Industry. 1-[3-(Dimethylamino)propyl]-3-ethylcarbodiimide hydrochloride (EDCI) was purchased from Aldrich. AIBN, ethyl acrylate, potassium carbonate, 4-iodobenzoic acid, and *t*-AmOH were purchased from Wako Pure Chemical Industry. Merrifield resin HL (1% DVB, 100–200 mesh) and *N*-methylaminomethyl polystyrene resin (**8**, 1% DVB, 100–200 mesh) were purchased from Novabiochem. ArgoPore Wang Resin was purchased from Argonaut. The glass used as a support was purchased from MATSUNAMI Glass. $\text{Pd}(\text{PPh}_3)_4$ and trifluoroacetic acid were purchased from Kanto Chemical. Dry solvents (THF, DCM, DMF) were purchased from Wako Pure Chemical Industry. Tetraethyleneglycol mono-2-phenyl-2-propenyl ether was prepared according to the literature.¹⁰ Column chromatography was performed on silica gel 60 (Merck), and preparative TLC was carried out by using Wakogel B-5F (Wako Pure Chemical Industry). XRF analysis was performed by Shimadzu EDX-800.

Microscopic Analysis. TEM images were obtained using a JEOL JEM-1200EX II instrument operated at 80 kV. TEM specimens of all, except for **6b**, were prepared by placing a drop of the solution on carbon-coated Cu grids and allowed to dry in air (without staining). For the TEM specimen of **6b**, a drop of the suspension of **6b** in MeOH, which was ground in a mortar with a pestle after freeze-drying with benzene, was placed on a Cu grid. SEM images were obtained using a Topcon LS-750 instrument operated at 10 kV. SEM specimens of all were coated with platinum for 60 s in a sputter coater (Polaron SC 7640).

X-ray Absorption Fine Structure. X-ray absorption experiments were carried out on the beam line 10B²⁶ at the Photon Factory at the High Energy Accelerator Research Organization Institute of Materials Structure Science (KEK-PF), Tsukuba, Japan, with a ring energy of 2.5 GeV and stored current of 450–380 mA. X-ray absorption spectra were recorded in a transmission mode at room temperature with a Si-(311) channel cut monochromator. The intensities of the incident and transmitted X-ray were measured with a 17-cm ion chamber with an Ar gas flow and a 62-cm ion chamber with an Ar gas flow, respectively. Energy calibration was carried out using the Pd K-edge of a Pd foil. The nonlinear curve-fitting analysis was performed for the Fourier-filtered EXAFS.

Preparation of Vinyl Monomer. 3-Bromo-2-phenylpropene.²⁷ The mixture of 2-phenylpropene (22.4 g, 190 mmol), NBS (23.7 g, 133 mmol), and bromobenzene (76 mL) was rapidly heated in an oil bath at 160 °C until the NBS was dissolving. After cooling to room temperature, the precipitate was removed by filtration and washed with chloroform. The filtrate was purified by distillation (bp 80–85 °C/3 mmHg) to afford 3-bromo-2-phenylpropene containing 1-bromo-2-phenylpropene (15.5 g). The purity was found to be 78.0% (determined by ^1H NMR). ^1H NMR (CDCl_3) $\delta = 4.39$ (s, 2H), 5.49 (s, 1H), 5.56 (s, 1H), 7.33–7.51 (m, 5H); ^{13}C NMR (CDCl_3) $\delta = 34.2$, 117.2, 126.1, 128.3, 128.5, 137.6, 144.2.

2-[(2-Phenylallyloxy)methyl]oxirane. To sodium hydride (60% in mineral oil, 1.6 g, 40 mmol) suspended in dry DMF (75 mL) was added glycidol (7.4 g, 100 mmol) in DMF (5 mL) at 0 °C. Then the solution of 3-bromo-2-phenylpropene (78% purity, 5.05 g, 20 mmol) in DMF

(10 mL) was added at the same temperature, and the mixture was stirred for 24 h at room temperature. After the mixture was cooled to 0 °C and diluted with diethyl ether, saturated aqueous ammonium chloride was added to quench the reaction, and the aqueous layer was then extracted with diethyl ether. The combined organic layers were dried over sodium sulfate, and the solvent was removed under reduced pressure. The residue was purified by silica gel column chromatography (hexane/EtOAc) to afford 2-[(2-phenylallyloxy)methyl]oxirane (2.66 g, 70%). ^1H NMR (CDCl_3) $\delta = 2.59$ (dd, 1H, $J = 2.7$, 5.1 Hz), 2.78 (dd, 1H, $J = 4.2$, 5.1 Hz), 3.13–3.17 (m, 1H), 3.46 (dd, 1H, $J = 5.8$, 11.5 Hz), 3.77 (dd, 1H, $J = 3.2$, 11.5 Hz), 4.41 (ddd, 1H, $J = 0.7$, 1.2, 12.9 Hz), 4.48 (ddd, 1H, $J = 0.5$, 1.2, 12.9 Hz), 5.34–5.36 (m, 1H), 5.53–5.54 (m, 1H), 7.45–7.48 (m, 5H); ^{13}C NMR (CDCl_3) $\delta = 44.3$, 50.8, 70.5, 73.2, 114.6, 126.0, 127.8, 128.4, 138.6, 143.9; IR (KBr) 3000, 2924, 2867, 1911, 1812, 1701, 1630, 1512, 1479, 1407, 1337, 1254, 1205, 1107, 991, 909, 839 cm^{-1} ; HRMS (EI): Calcd for $\text{C}_{13}\text{H}_{16}\text{O}_2$ (M^+), 190.0994; found, 190.0998.

Preparation of Copolymer (2). Styrene (7.53 g, 72.3 mmol), 2-[(2-phenylallyloxy)methyl]oxirane (1.72 g, 9.04 mmol), tetraethyleneglycol mono-2-phenyl-2-propenyl ether (2.81 g, 9.04 mmol), and AIBN (105.9 mg, 0.65 mmol) were mixed in chloroform (11.5 mL). The mixture was stirred for 48 h at reflux and then cooled to room temperature. The resulting polymer solution was poured slowly into methanol. The precipitated polymer was filtered and washed with methanol several times and dried for 24 h under reduced pressure to afford the desired copolymer (**2**, 7.35 g, 61% yield). The molar ratio of the components was determined by ^1H NMR analysis ($x/y/z = 91:5:4$). M_w : 31 912, M_n : 19 468, $M_w/M_n = 1.64$ (gel permeation chromatography).

Preparation of Pd-Containing Polymer Micelles. Pd-Containing Polymer Micelle (4). Copolymer (**2**, 500 mg) and $\text{Pd}(\text{PPh}_3)_4$ (500 mg, 0.43 mmol) were dissolved in DCM (10 mL), and *t*-AmOH (50 mL) was then slowly added. The mixture was stirred for 8 h at room temperature to form polymer micelles. The micelle solution was heated for 5 h at 120 °C in a sealed tube to cross-link the polymer side chain, and then the micelle solution was poured into MeOH. The precipitate was collected by filtration and dried to afford Pd-containing spherical polymer micelle (**4**, 534 mg, Pd = 0.81 mmol/g).

Pd-Containing Polymer (5), Cross-Linked by Microwave Irradiation. Copolymer (**2**, 50 mg) and $\text{Pd}(\text{PPh}_3)_4$ (50 mg, 0.04 mmol) were dissolved in DCM (1 mL), and *t*-AmOH (5 mL) was then slowly added. The mixture was stirred for 8 h at room temperature to form polymer micelles. The micelle solution was heated at 120 °C for 1 h in a sealed tube by MW irradiation, and the mixture was then poured into MeOH. The precipitates were collected by filtration and dried to afford Pd-containing polymer (**5**, 24.9 mg, Pd = 1.73 mmol/g).

Pd-Containing Polymer Micelle (6a). Copolymer (**2**, 2.0 g) and $\text{Pd}(\text{PPh}_3)_4$ (2.0 g, 1.72 mmol) were dissolved in THF (40 mL), the mixture was stirred for 8 h at room temperature, and then hexane (120 mL) was added slowly. The precipitates were collected by filtration and dried, and then the solid was heated for 2 h at 120 °C without solvents. The resulting solid was washed with THF and DCM, successively, and the insoluble Pd-containing solid (**6a**, 1.90 g, Pd = 0.65 mmol/g) was obtained.

Pd-Containing Polymer Micelle (6b). Copolymer (**2**, 500 mg) and $\text{Pd}(\text{PPh}_3)_4$ (500 mg, 0.43 mmol) were dissolved in DCM (10 mL), the mixture was stirred for 8 h at room temperature, and then MeOH (30 mL) was added slowly. The precipitates were collected by filtration and dried, and then the solid was heated for 2 h at 120 °C without solvents. The resulting solid was washed with THF, NMP, and DCM, successively, and the insoluble Pd-containing solid (**6b**, 440 mg, Pd = 0.62 mmol/g) was obtained.

Pd-Containing Polymer Micelle on Glass (9). Copolymer (**2**, 200 mg) and $\text{Pd}(\text{PPh}_3)_4$ (200 mg, 0.17 mmol) were dissolved in DCM (20 mL), and *t*-AmOH (100 mL) was slowly added to this mixture to form polymer micelles. To this solution, glass (microscope cover glass, borosilicate glass (SiO_2 64.2%, B_2O_3 8.9%, Na_2O 7.2%, ZnO 7.1%, K_2O

(26) Nomura, M.; Koyama, A. *KEK Rep.* **1989**, 89–16, 21.

(27) (a) Reed, S. F., Jr. *J. Org. Chem.* **1965**, 30, 3258. (b) Vaccher, C.; Berthelot, P.; Flouquet, N.; Vaccher, M.-P.; Debaert, M. *Synth. Commun.* **1993**, 23, 671–679.

6.4%), 18 × 18 mm, washed with 1 N NaOH aq/EtOH (1/1), water, and EtOH, successively, before use) was added, and the mixture was allowed to stand overnight to precipitate the micelles onto the glass. The glass with micelles was washed with MeOH and dried and then heated for 2 h at 120 °C. The resulting glass was washed with THF and DCM, successively, and Pd-containing polymer micelles on glass (**9**) were obtained.

Hydroxylated Resin (7). To sodium hydride (60% in mineral oil, 4.6 g, 115 mmol) suspended in THF (150 mL) was added tetrethrenglycol (22.3 g, 115 mmol) at 0 °C. The mixture was stirred for 1 h at this temperature. Then Merrifield resin HL (1% DVB, 100–200 mesh, 10 g) was added at the same temperature, and the mixture was then stirred for 24 h at room temperature. After the mixture was cooled to 0 °C, saturated aqueous ammonium chloride was added to quench the reaction. The resin was filtered and washed successively with THF, water, MeOH, THF, and DCM. The resulting resin was dried to afford hydroxylated resin (**7**, 10.2 g). IR (KBr) 3440, 3059, 3026, 2922, 2858, 1946, 1603, 1493, 1452, 1352, 1099, 819, 760, 700, 541 cm⁻¹.

Pd-Containing Polymer Micelle on Hydroxylated Resin (10, 10L). Copolymer (**2**, 200 mg) and Pd(PPh₃)₄ (200 mg, 0.17 mmol) were dissolved in DCM (20 mL), and *t*-AmOH (100 mL) was slowly added to this mixture to form polymer micelles. To this solution, hydroxylated resin (**7**, 2.0 g for **10**, 10.0 g for **10L**) was added, and the mixture was allowed to stand overnight to precipitate the micelles onto the resin. The resin with micelles was washed with MeOH and dried and then heated for 2 h at 120 °C. The resulting resin was washed successively with THF and DCM and dried to afford Pd-containing polymer micelles on hydroxylated resin (**10**, 1.73 g, Pd = 0.009 mmol/g, **10L**, 9.80 g, Pd = 0.0008 mmol/g).

Pd-Containing Polymer Micelle on Aminated Resin (11). Copolymer (**2**, 200 mg) and Pd(PPh₃)₄ (200 mg, 0.17 mmol) were dissolved in DCM (20 mL), and to this mixture was then slowly added *t*-AmOH (100 mL) to form polymer micelles. To this solution, *N*-methylaminomethyl polystyrene resin (**8**, 1% DVB, 100–200 mesh, 2.0 g) was added, and the mixture was allowed to stand overnight to precipitate the micelles onto resin. The resin with micelles was washed with MeOH and dried and then heated for 2 h at 120 °C. The resulting resin was washed successively with THF and DCM and dried to afford Pd-containing polymer micelles on aminated resin (**11**, 1.52 g, Pd = 0.037 mmol/g).

Determination of Loading of the Pd. The Pd-containing sample (50.0 mg) was placed in a 50-mL test tube, and sulfuric acid (1.0 mL) was added. The mixture was heated at 180 °C for 30 min, and then nitric acid (0.5 mL) was added. The mixture was further heated for 1 h to give a clear solution. The solution was diluted with water, and the amount of Pd metal was measured by XRF analysis.

Quantitative Analysis of Surface Hydroxy Groups. **6a** and **6b** were converted to the corresponding urethane derivatives, and amine cleavage and subsequent photometrical quantitative analysis revealed the total amount of the generated and remaining surface hydroxy groups of **6a** and **6b**. The networked Pd-containing polymer micelle (**6a** or **6b**, 100 mg) and α -naphthylisocyanate (700 mg, 4.14 mmol) were combined in toluene (10 mL) and stirred for 24 h at 45 °C. The urethanated polymer micelle solid was collected by filtration and was washed well with toluene and MeOH. The solid was dried under reduced pressure and then heated for 24 h at 50 °C in 1 N NaOH (5.0 mL). After cooling to room temperature, 1 N HCl (5.0 mL) was added and the solid was removed by filtration and then washed with pure water. The filtrate volume was adjusted to 100 mL, the UV–visible spectrum was recorded (Shimadzu UV-1650PC), and the amount of liberated α -naphthylamine ($\lambda_{\text{max}} = 277.6$ nm, $\epsilon_{\text{max}} = 5884.3$) in the filtrate was calculated from the absorbance at 277.6 nm. The total amounts of the generated and remaining surface hydroxy groups were determined to be 1.1 $\mu\text{mol/g}$ for **6a** and 117.8 $\mu\text{mol/g}$ for **6b**.

Hydrogenation and Heck Reaction Catalysis. Hydrogenation of Quinoline Using Pd-Containing Polymer Micelle (6b). Pd-containing

polymer micelles (**6b**, 40.3 mg, 0.025 mmol) and quinoline (64.6 mg, 0.50 mmol) were combined in THF (5 mL). The mixture was stirred for 24 h at room temperature under hydrogen (1 atm). The catalyst was filtered and washed with THF, and the solvent of the filtrate was removed under reduced pressure. The residue was purified by PTLC to afford 1,2,3,4-tetrahydroquinoline (67.0 mg, quantitatively). **1,2,3,4-Tetrahydroquinoline.**²⁸ ¹H NMR (CDCl₃) $\delta = 1.87$ – 1.95 (m, 2H), 2.76 (t, 2H, $J = 6.4$ Hz), 3.24–3.28 (m, 2H), 3.70 (brs, 1H), 6.44 (d, 1H, $J = 7.7$ Hz), 6.58 (t, 1H, $J = 7.5$ Hz), 6.91–6.97 (m, 2H); ¹³C NMR (CDCl₃) $\delta = 22.2$, 27.0, 41.9, 114.1, 116.8, 121.3, 126.7, 129.4, 144.8.

A Typical Procedure for a Heck Reaction Using Pd-Containing Polymer Micelles. Pd-containing polymer micelles (**6b**, 5 × 10⁻⁴ mmol), iodobenzene (10.2 g, 50 mmol), ethyl acrylate (7.5 g, 75 mmol), and potassium carbonate (13.8 g, 100 mmol) were combined in NMP (50 mL). The mixture was stirred for 24 h at 120 °C. The catalyst was filtered and washed with THF, and the solvents of the filtrate were removed under reduced pressure. The residue was extracted with diethyl ether three times, the combined organic layers were washed with water and dried over sodium sulfate, and the solvent was removed under reduced pressure. The residue was purified by silica gel column chromatography to afford ethyl *trans*-cinnamate (7.3 g, 83%). **Ethyl *trans*-Cinnamate.** ¹H NMR (CDCl₃) $\delta = 1.34$ (t, 3H, $J = 7.1$ Hz), 4.27 (q, 2H, $J = 7.1$ Hz), 6.44 (d, 1H, $J = 15.6$ Hz), 7.36–7.39 (m, 3H), 7.51–7.53 (m, 2H), 7.69 (d, 1H, $J = 15.6$ Hz); ¹³C NMR (CDCl₃) $\delta = 14.3$, 60.5, 118.3, 128.0, 128.9, 130.2, 134.5, 144.6, 167.0.

Wang Resin-Bound Iodobenzoic Acid.²³ Wang Resin (ArgoPore-Wang, 0.54 mmol/g, 189 μm , ave) was washed successively with DCM and EtOH and dried for 24 h in vacuo before use. The resin (10 g, 5.4 mmol), 4-iodobenzoic acid (6.7 g, 27 mmol), and 4-(dimethylamino)pyridine (0.33 g, 2.7 mmol) were combined in dry DMF (100 mL). To this mixture EDCI (5.18 g, 27 mmol) was added at 20 °C, and the mixture was then stirred at 60 °C for 12 h. Resin was filtered and washed successively with DCM, MeOH, water, MeOH, and DCM. The resulting resin was dried to afford Wang Resin-bound iodobenzoic acid (11.2 g). A portion of this resin (0.5 g) was treated with TFA/DCM (6 mL/2 mL) at room temperature for 1 h, and resin was removed by filtration. The filtrate was evaporated in vacuo to afford iodobenzoic acid (55.0 mg). The loading of iodobenzoic acid on Wang Resin was therefore determined to be 0.444 mmol/g. ¹H NMR (DMSO-*d*₆) $\delta = 3.42$ (brs, 1H), 7.68 (d, 2H, $J = 7.3$ Hz), 7.88 (d, 2H, $J = 7.3$ Hz); ¹³C NMR (CDCl₃) $\delta = 101.2$, 130.2, 131.1, 137.6, 166.9.

Three-Phase Test. Pd-containing polymer micelles (**6b**, 8.9 × 10⁻⁵ mmol), Wang Resin-bound iodobenzoic acid (2.0 g, 0.89 mmol), ethyl acrylate (133.7 mg, 1.34 mmol), and potassium carbonate (246.0 mg, 1.78 mmol) were combined in NMP (10 mL). The mixture was stirred for 24 h at 120 °C. The mixture was filtered and washed successively with THF, water, EtOH, and DCM and then dried for 24 h in vacuo. The resulting resin was treated with TFA/DCM (24 mL/8 mL) at room temperature for 1 h. The resin was removed by filtration and washed with EtOH and DCM. The filtrate was evaporated in vacuo and analyzed by ¹H NMR spectroscopy using durene as an internal standard. The liberated 4-(2-ethoxycarbonyl-vinyl)-benzoic acid was calculated from the ¹H NMR spectrum to be 4.39 mg (2% yield).

Conclusion

It was demonstrated that subnanometer Pd clusters were formed in polymer micelles by ligand exchange from Pd(PPh₃)₄ and that the micelle morphologies were frozen into spherical, rodlike, and 3-D networked micelles by cross-linking. These micelles containing ultrafine Pd clusters not only have high potential as catalysts but also would serve as nanoreactors and can create several nanoarchitectures. Moreover, the fixation

(28) Sanchez-Delgado, R. A.; Gonzalez, E. *Polyhedron* **1989**, *8*, 1431–1436.

method of the micelle catalysts onto several supports such as glass surfaces and resins could be applied to flow system reactors. Since several other metals can be immobilized by similar methods,⁹ such micelles including ultrafine metal clusters allow for the future development of high-performance materials in diverse fields.

Acknowledgment. This work was partially supported by CREST, SORST, ERATO, Japan Science and Technology

Agency (JST), and a Grant-in-Aid for Scientific Research from Japan Society of the Promotion of Science (JSPS). The X-ray absorption experiments were performed under the approval of the Photon Factory Program Advisory Committee (Proposal No. 2003G250). We are grateful to Dr. John S. Fossey (The University of Tokyo) who read our manuscript very carefully and gave us several helpful suggestions.

JA047095F